

Electron Measurements with the High Energy Particle Calorimeter Telescope (HEPCaT)

J.W. Mitchell*, T. Hams^{*,1}, J.F. Krizmanic^{*,2}, A.A. Mosieev^{*,3}, M. Sasaki^{*,3},
R.E. Streitmatter*, J.H. Adams[†], M.J. Christl[†], J.W. Watts[†], T.G. Guzik[‡], J. Isbert[‡],
J.P. Wefel[‡], C.B. Cosse[§], and S.J. Stochaj[§]

*NASA/GSFC, Greenbelt, MD 20771, USA

†NASA/MSFC, Huntsville, AL 35812, USA

‡Louisiana State University, Baton Rouge, LA 70803, USA

§New Mexico State University, Las Cruces, NM 88003, USA

Abstract. HEPCaT is designed to make direct measurements of cosmic-ray electrons to energies above 10 TeV, as part of the Orbiting Astrophysical Spectrometer in Space (OASIS) mission under study by NASA as an Astrophysics Strategic Mission Concept. These measurements have unmatched potential to identify high-energy particles accelerated in a local astrophysical engine and subsequently released into the Galaxy. The electron spectrum may also show signatures of dark-matter annihilation and, together with Large Hadron Collider measurements, illuminate the nature of dark matter. HEPCaT uses a sampling, imaging calorimeter with silicon-strip-detector readout and a geometric acceptance of $2.5 \text{ m}^2 \text{ sr}$. Powerful identification of the abundant hadrons is achieved by imaging the longitudinal development and lateral distribution of particle cascades in the calorimeter. A neutron/penetration detector provides additional hadron rejection by measuring the neutron flux and the number of penetrating cascade particles. A silicon pixel detector measures particle charge and identifies gamma rays. HEPCaT will extend direct electron and hadron measurements to higher energies than any current or planned instrument.

Keywords: galactic cosmic ray, high energy electrons, OASIS

I. INTRODUCTION

The High Energy Electron Calorimeter Telescope (HEPCaT) is one of the two instruments that make up the OASIS mission [1]. The two HEPCaT modules, shown in Figure 1, use ionization calorimetry to extend measurements of high energy cosmic-ray electrons to above 10 TeV. HEPCaT combines a large geometric factor, $2.5 \text{ m}^2 \text{ sr}$, with excellent energy resolution, $<10\%$ at 1 TeV, and the ability to eliminate contamination of the electron spectrum by the far more abundant protons.

Direct HEPCaT observation of high-energy Galactic cosmic-ray (GCR) electrons could identify with unprecedented sensitivity the signature of high-energy particles released into the Galaxy from a local astrophysical accelerator. High-energy electrons and positrons may also

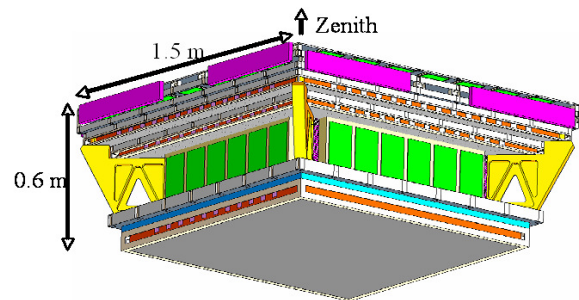


Fig. 1: One HEPCaT Module.

be produced by dark-matter annihilation. Details of the spectra and anisotropy of high-energy cosmic-ray electrons, combined with measurements at the Large Hadron Collider and measurements of high-energy positron and antiproton spectra, may hold the key to revealing the nature of the ubiquitous, but little understood, dark matter. Recent releases of data from ATIC [2], PAMELA [3], HESS [4], and Fermi-LAT [5] have generated tremendous interest in high-energy electrons and around 200 interpretation papers have been introduced in the past year. Only a few are discussed below.

HEPCaT will measure the secondary to primary ratios of nuclear cosmic rays to above 10^{14} eV , including B/C and sub-Fe/Fe, providing important data to test models of cosmic-ray transport including the energy dependence of the matter traversed. HEPCaT will also measure the spectra of individual elements, H to Ni, to above 10^{15} eV where charge-dependent spectral cutoffs, leading to the "knee" in the cosmic-ray all-particle spectrum, may be observed.

II. HIGH ENERGY ELECTRONS

Observations of radio and non-thermal X-ray emission, and recent measurements of TeV γ -rays, provide evidence that particles are accelerated to energies $>1 \text{ TeV}$ in supernova remnants (SNR). Similarly, there is ample evidence that high-energy electrons are accelerated in pulsars and pulsar wind nebulae. However, there is no direct evidence that particles escape these sources.

¹Also University of MD Baltimore County, Baltimore, MD.

²Also University of MD, Collage Park, MD.

³Also Universities Space Research Association, Columbia, MD.

High-energy GCR electrons provide a unique probe of local cosmic accelerators because their rapid energy loss by synchrotron and inverse Compton processes suppresses the flux from distant sources. The electron spectrum from the superposition of distant sources is expected to be relatively featureless, falling approximately as E^{-3} and softening rapidly above 1 TeV. This is illustrated in Figure 2 which shows recent experimental data on the high energy electron spectrum together with a model of the net contribution of distant sources. The electron lifetime, and so the distance they can diffuse in that time, decreases rapidly with energy. Electrons with TeV energies must have been accelerated within $\sim 10^5$ yrs of their detection and can have diffused at most a few hundred pc [6,7]. Thus, electrons with energy significantly above 1 TeV would indicate a nearby source and should show significant anisotropy in their arrival directions [6].

A. Astrophysical Sources of High-Energy Electrons

Features from discrete sources may be visible in the high-energy cosmic-ray electron spectrum [7] above the distant-source cutoff, as illustrated in Figure 2. Results from HESS [4] show the expected cutoff, but indicate that the spectrum may recover and extend to well above 1 TeV. A feature might also be superimposed on the spectrum. ATIC reported such a feature [2] at ~ 600 GeV. It has been argued [8,9] that a combination of known pulsars injecting high energy e^+ and e^- is the most likely explanation for both the ATIC feature and the positron excess measured by PAMELA [3]. The Large Area Telescope on the Fermi Gamma-ray Space Telescope (Fermi-LAT) recently reported the electron spectrum measured to 1 TeV [5]. As shown in Figure 2, the Fermi-LAT data do not reproduce the sharpness of the ATIC feature, but show a harder spectrum than predicted by standard models and may also indicate an excess. ATIC has $\sigma \sim 2\%$ energy resolution but with statistics limited by its exposure. Fermi-LAT has great statistical precision but a thinner calorimeter and energy resolution of $\sigma \sim 8.5\%$ at 600 GeV ($\sim 20\%$ FWHM reported). At the time of writing, the differences between the two measurements were under discussion. In addition, recent HESS results show a spectrum similar to Fermi-LAT [10]. Exploiting the full potential to investigate local accelerators requires an instrument that can accurately measure the electron spectrum and arrival directions to at least 10 TeV. Current instruments, ATIC ($0.16 \text{ m}^2\text{sr}$), PAMELA ($0.0021 \text{ m}^2\text{sr}$), Fermi-LAT ($1 \text{ m}^2\text{sr}$ at 1 TeV), and AMS (calorimeter $0.06 \text{ m}^2\text{sr}$) are limited to ~ 1 TeV either by their instrumentation (calorimeter depth or spectrometer maximum detectable rigidity) or by exposure. In contrast, the HEPCaT instrument is optimized for high-energy electron measurements to above 10 TeV, with $\sim 7.5 \text{ m}^2\text{sr yr}$ of exposure, proton rejection efficiency $> 10^4:1$, and energy resolution $\sigma < 10\%$.

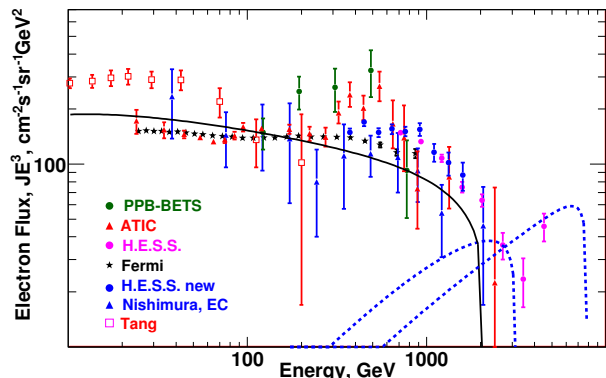


Fig. 2: Current high energy electron data. Solid line is $E^{-3.27}$ with a cutoff at 2 TeV. Dashed lines suggest spectral contributions from individual sources.

B. Electron signatures of Dark-Matter Annihilation

High-energy electrons may also result from annihilation of candidate dark-matter (DM) particles, including weakly interacting massive particles (WIMP) predicted by supersymmetric (SUSY) theories (neutralinos) or Kaluza-Klein (KK) particles predicted by theories involving compactified extra dimensions. A DM source would be seen as excess flux up to the DM rest mass with a spectral shape that depends on the candidate particle and its annihilation channels. To fit ATIC [2] and PAMELA [3] data, DM annihilation must produce a hard lepton spectrum near the DM rest mass directly or from decay of intermediate particles. For annihilations throughout the Galactic halo, this suggests that DM must annihilate mainly into charged leptons [11]. ATIC and PAMELA features may also require either much larger annihilation cross-sections than predicted by models for the WMAP "haze" or local "clumps" of dark matter that could lead to a "boost" in the flux of e^+ and e^- measured at Earth [12]. The Fermi-LAT data reduce this requirement [13]. ATIC [2] reported a good fit to their data from annihilation of 620 GeV rest mass KK particles, which can annihilate directly into e^+ and e^- , producing a distinctive feature with a sharp high-energy cutoff at the KK rest mass [14]. In contrast, neutralinos are generally thought to annihilate preferentially into quarks and gauge bosons (e.g. W^+W^-), with little or no direct e^+e^- channel, and subsequent boson decays produce electrons distributed over a range of energies. Propagation processes further distribute the electrons to lower energy. Mechanisms for WIMP annihilation that produce hard leptons through decay of light intermediate bosons have also been proposed [15]. Spectral shape alone is not sufficient to discriminate between DM annihilations and a nearby pulsar source, and measured arrival directions will be important [16]. DM annihilation throughout the halo might produce a small dipole anisotropy in the direction of the Galactic center. A localized source such as a local DM clump or a pulsar might produce a different anisotropy. Additional constraints to DM models come from antiprotons [17,18]

and diffuse γ -ray emission.

III. HIGH ENERGY NUCLEAR SPECTRA

HEPCaT uses a calorimeter that is very deep by spaceflight standards, giving nearly two hadron interaction lengths and an energy resolution of about 40%, limited mainly by shower leakage. HEPCaT is capable of measuring energy spectra of high-energy nuclei, H to Ni, limited only by exposure. This enables it to address important aspects of the acceleration and transport of cosmic-ray nuclei in the Galaxy.

A. Nuclear Secondary to Primary Ratios

GCR primary nuclei originate in the source while secondaries, such as boron, are produced by the spallation of heavier nuclei during propagation through the ISM. Thus, the B/C ratio is a measure of the amount of matter traversed by GCR nuclei. The B/C ratio is observed to decrease with increasing energy, indicating that higher energy GCRs spend less time in the galaxy before escaping, with an energy-dependent path-length proportional to $\sim E^{-0.6}$. This trend would be limited at higher energies if the GCR sources are shrouded. Evidence that GCR sources are shrouded by dense stellar winds or super-bubble shells [18] would, in turn, be an indication that GCRs come from OB associations. Measurement of the energy dependence of the B/C ratio up to ~ 5 TeV would determine whether this ratio continues as $E^{-0.6}$ or has a flatter energy dependence [18] at higher energies because the GCRs must traverse a minimum path length in shrouds before escaping their source regions.

B. High-Energy Charge-Dependent Spectral Cutoffs

High-energy cutoffs in the GCR elemental energy spectra would provide strong support for the SNR acceleration model [19], but have yet to be observed. To reach the energies where these cutoffs are expected requires long exposures only possible with a space experiment. This was the goal of ACCESS. HEPCaT will measure individual elemental spectra, H to Ni, to energies $>10^{15}$ eV where charge-dependent spectral cutoffs may be observed, testing models of GCR acceleration and providing important calibration data for ground airshower arrays.

IV. TECHNICAL OVERVIEW

The High Energy Particle Calorimetry Telescope (HEPCaT) uses ionization calorimetry to measure electrons at energies from a few GeV to above 10 TeV and GCR H to Ni to >1000 TeV. HEPCaT unambiguously distinguishes electrons from the $\sim 10^4$ times more abundant protons. Its highest energy is limited only by geometric acceptance and exposure. HEPCaT incorporates an imaging, sampling silicon tungsten-calorimeter (STC) to measure particle energy and distinguish electrons from hadrons, a silicon-pixel charge identification detector (CID) to measure electric charge and identify

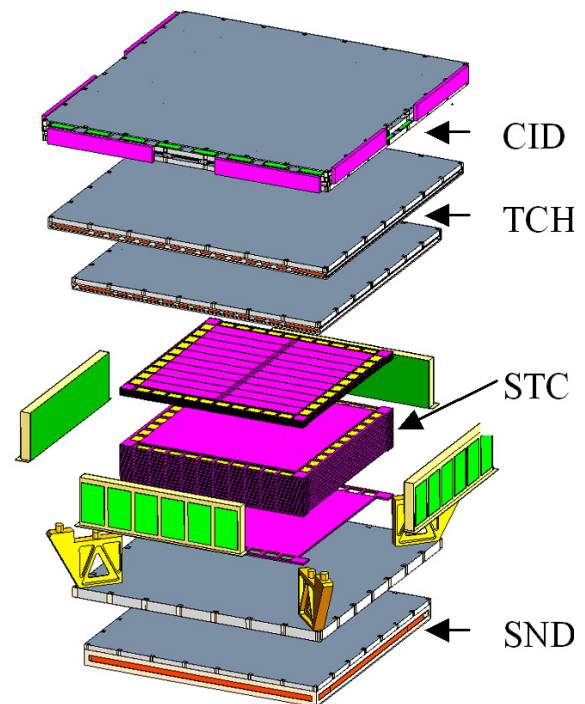


Fig. 3: Expanded view of one HEPCaT module

γ -rays, a plastic scintillator trigger/charge hodoscope (TCH) array for triggering, and a secondary neutron detector (SND) to detect neutrons and penetrating showers, contributing to electron/hadron separation. Identical zenith-pointing modules with geometric factors of over $1.25 \text{ m}^2 \text{ sr}$ are located on either side of the OASIS spacecraft giving an exposure of $7.5 \text{ m}^2 \text{ sr yr}$ in a three-year mission. An energy resolution of $<10\%$ at energies above a few hundred GeV allows precise measurement of spectral features. Figures 1 and 3 show one HEPCaT module. Important HEPCaT parameters are given in Table 1.

All HEPCaT technologies have heritage from accelerator, ground-based and balloon-borne instruments. They have also been flown in space. Ionization calorimetry is a standard technique for measuring electron and hadron energies and is central to most major accelerator experiments. High-energy GCR calorimetry was pioneered in the Proton satellites [21]. In the ACCESS study, NASA simulated and tested prototypes of the detectors proposed for HEPCaT using 10 to 375 GeV hadrons, electrons, and nuclei. The simulation effort has been expanded during the OASIS study. HEPCaT can be implemented using current detector and electronic components.

Ionization calorimeters determine incident particle energy by measuring the energy deposited in a massive absorber by particle cascades (showers). The energy of the particle can be determined even if the shower is not fully contained within the calorimeter, although resolution is reduced. Cascade development is characterized by an interaction length (λ_I) for hadrons and radiation length (X_0) for electrons and photons. In dense materials, λ_I

Performance Parameter:	Required	Expected
Exposure factor [m ² sr yr]	6	7.5 (3 yr)
e energy range [TeV]	0.01 – 10	0.01 – 30
Charge resolution	0.2e 1 ≤ Z ≤ 26	0.15e 1 ≤ Z ≤ 26
e/γ energy resolution 1 TeV	<20%	<10%
p energy resolution 1000 TeV	<50%	<40%
e/p separation	10 ⁻⁵	< 10 ⁻⁵
RMS position at CID	<5 mm	<3 mm
Field-of-view	60°	60°

TABLE I: HEPcAT Performance Parameters.

is much larger than X_0 . To meet the OASIS goals, a calorimeter is needed that fully contains electromagnetic showers but may not fully contain hadronic showers. Electromagnetic showers peak quickly, and the particle number drops to $\sim 1\%$ of peak after $\sim 30 X_0$ even at the highest HEPcAT energies. Simulations and scaling from CERN tests show that the STC will have an energy resolution of $<10\%$ at 1 TeV for electrons and photons, improving to $<3\%$ at 10 TeV. Hadronic showers are more complicated and shower leakage from the STC limits the energy resolution. For hadrons, the STC will have $<40\%$ resolution at 1000 TeV.

HEPcAT distinguishes electrons from hadrons using a combination of shower characteristics, including the longitudinal and transverse shower profile in the STC and both charged particles and neutrons detected in the SND. The STC detectors have fine transverse segmentation and are sensitive to singly-charged particles. Electron showers start in the STC before proton showers and are almost fully contained after $\sim 30 X_0$ while most proton showers deposit energy deeper. Electron showers are extremely narrow. The proton showers have a narrow core surrounded by a halo. The separation techniques used have been proven at accelerators and by experience with PAMELA [22], ATIC [23], and Fermi-LAT [24].

STC: The STC uses 32 interleaved silicon strip detector (SSD) layers and tungsten absorber plates giving $40 X_0$ and $1.7 (\lambda_I)$ in an active volume $0.83\text{m} \times 0.83\text{m} \times 0.38\text{m}$. The absorber thicknesses are graduated, becoming thicker with depth, based on the space-proven PAMELA calorimeter design [25]. The single-sided SSDs are $8\text{cm} \times 8\text{cm} \times 380\mu\text{m}$, with 32 anode strips on a 2.4 mm pitch. One hundred SSDs make up each detector layer. The SSDs detect individual minimum-ionizing singly-charged particles up to the shower maximum of 10^{15} eV events requiring a dynamic range of $\sim 10^7$, achieved by reading out both sides of the SSD using conventional electronics with a range of $\sim 10^4$.

CID: The CID, derived from the ATIC [23] design, uses a double layer of silicon pixel detectors with a charge resolution of 0.15 - 0.2 e. To avoid confusion from shower albedo, the pixels are 1cm^2 . Particle showers in the STC point back to the entrance pixel. Each CID layer is a mosaic of $\sim 21,000$ pixels in arrays of $10\text{cm} \times 10\text{cm}$ detectors. Detectors are partly overlapped and the layers staggered for full coverage.

TCH: Each TCH module has two orthogonal layers of

scintillator strips read out at each end by PMTs whose signals are electronically discriminated to provide fast triggers. Pulse amplitudes are read by time-sampling electronics to separate incident particles from albedo.

SND: The SND uses borated plastic scintillators with PMT readout. Charged shower particles and neutrons are distinguished by their arrival times since fast neutrons are delayed by thermalization. Shower particles are read within ~ 100 ns after a trigger. SND pulses are then counted to give the number of detected neutrons. SND can reject $\sim 95\%$ of hadronic showers.

Electronics: Readout electronics for all detectors use commercial ASICs. Signals from the TCH, the high-energy range on the STC ladders, and the SND give trigger information. Triggers for electrons, p/He, heavier nuclei, and γ -rays can be used simultaneously. Computed triggers (L1) select a total energy threshold and provide scale-down factors. Following a L0 trigger, data is gathered from each readout board by local FPGA-based data handlers and transmitted to the central CPU, which applies L1 triggers and builds the event for transmission to the spacecraft. With a 10 GeV electron - 100 GeV hadron threshold, the event rate is $\sim 24/\text{s}$.

V. SUMMARY

The HEPcAT instrument on the OASIS mission has the exposure, background rejection, and energy resolution needed to investigate particle acceleration in local astrophysical engines using high energy electrons. HEPcAT will also search the electron spectra for signatures of dark-matter annihilations. In addition, HEPcAT will search for high-energy spectral cutoffs, as evidence of SNR acceleration of GCR nuclei, and will measure GCR nuclear secondary to primary ratios to high energy, as input to transport models.

REFERENCES

- [1] M. Christl *et al.* 2009, The Orbiting Astrophysical Spectrometer in Space (OASIS), Proc. 31st ICRC (Łódź)
- [2] J. Chang *et al.* 2008, Nature, 456, 362
- [3] O. Adriani *et al.* 2009, Nature 458, 607
- [4] F. Aharonian *et al.* 2008, Phys. Rev. Lett., 101, 261104
- [5] A.A. Abdo *et al.* 2009, Phys. Rev. Lett. 102, 181101
- [6] V.S. Ptuskin *et al.* 1995, Proc. 24th ICRC (Rome), 3, 56
- [7] T. Kobayashi *et al.* 2004, Astrophys. J., 601, 340
- [8] S. Profumo 2008, arXiv: 0812.4457v1
- [9] D. Hooper *et al.* 2009, J. Cosmology and Astropart. Phys., 1, 25
- [10] K. Egberts *et al.* 2009, 2nd Roma International Conference on Astro-Particle Physics (Rome), and private communication
- [11] I. Cholis 2008, arXiv:0809.1683
- [12] D. Hooper, A. Stebbins, and K.M. Zurek 2008, arXiv:0812.3202
- [13] D. Grasso *et al.* 2009, arXiv:0905.0636
- [14] D. Hooper and K.M. Zurek 2009, arXiv:0902.0593
- [15] I. Cholis 2008, arXiv:0811.3641
- [16] M. Pohl 2009, Phys. Rev., D79, 041301
- [17] Abe, K. *et al.* 2008, Phys. Lett. B 670, 103-108
- [18] O. Adriani *et al.* 2009, Phys. Rev. Lett. 102, 051101
- [19] M. Garcia-Munoz *et al.* 1987, ApJ Suppl., 64, 269
- [20] J.P. Meyer *et al.* 1997, ApJ, 487, 182 D.C. Ellison *et al.* 1997, ApJ, 487, 197,
- [21] V.V. Akimov *et al.* 1969, Proc. 11th ICRC (Budapest), 2, 211
- [22] P. Picozza *et al.* 2007, Astroparticle Phys. 27, 296
- [23] T.G. Guzik *et al.* 2004, Adv. Space Res. 33, 1763
- [24] H.F.-W. Sadrozinski *et al.* 2001, NIM, A466, 292
- [25] M. Boezio *et al.* 2002, NIM, A487, 407